

Ratio of σ_L/σ_T for $p(e, e'K^+)\Lambda$ Extracted from Polarization Transfer

Brian A. Raue*

Florida International University, Miami, FL 33199

Daniel S. Carman†

Ohio University, Athens, OH 45701

(Dated: May 22, 2019)

Abstract

The ratio of longitudinal to transverse structure functions, σ_L/σ_T , has been extracted from recent beam-recoil transferred polarization data for the $p(\vec{e}, e'K^+)\vec{\Lambda}$ reaction. Results have been obtained for $W=1.69, 1.84,$ and 2.03 GeV at an average Q^2 of 0.69 GeV². Our results indicate a ratio approaching zero. This is in contradiction to previously published results using a Rosenbluth separation. A similar difference between Rosenbluth and recoil polarization results has been observed in the measurement of the ratio of electric to magnetic form factors of the proton, $\mu_p G_E/G_M$.

PACS numbers: 13.40.-f, 13.60.Rj, 13.88.+e, 14.20.Jn, 14.40.Aq

*Electronic address: baraue@fiu.edu

†Electronic address: carman@ohio.edu

I. INTRODUCTION

Data taken in Hall B at Jefferson Laboratory have recently been published on polarization transfer in the reaction $p(\vec{e}, e'K^+)\vec{\Lambda}$ [1]. While these data have been used to shed light on the $s\bar{s}$ quark pair creation operator in the associated strangeness production reaction, they cannot yet provide direct constraints on the isobar models commonly employed to describe the reaction mechanism [2]. These phenomenological models (e.g.[3, 4]) rely on fitting the available data to provide constraints on the contributing intermediate-state resonant and non-resonant processes in the s , t , and u reaction channels. The models differ in the set of specific resonant states included, as well as in their treatment of hadronic form factors and the restoration of gauge invariance. However, due to the sparsity of data for this reaction and the large number of parameters in the models, the contributions to the intermediate state remain largely unconstrained and, therefore, are highly uncertain.

The new polarization transfer data are difficult to include in fitting the isobar model parameters. This is due to the fact that, by necessity, these data were averaged over a large range in momentum transfer Q^2 (0.3 to 1.5 GeV²) and a large range in the invariant energy W (~ 200 MeV bins). The data have also been averaged over all Φ , the angle between the electron scattering plane and the $K^+\Lambda$ hadronic reaction plane (Fig. 1). One could expect significant variations in the model parameters over such large kinematic ranges. This means that including these data, say at their central kinematic values, into a global refit of the parameters is improper. Therefore these data have been employed only as a cross check of the model parameters based on fits to the other measured observables.

The transferred polarization data can, however, provide useful new direct constraints to the models when they are used to extract the ratio of longitudinal to transverse structure functions, $R_\sigma = \sigma_L/\sigma_T$. This ratio has been previously measured using a Rosenbluth separation [5, 6, 7]. The results presented here provide a means of extracting R_σ that is less prone to systematic uncertainties than the Rosenbluth method and give markedly different results. This could signal the importance of such processes as two-photon exchange mechanisms in the interaction.

II. FORMALISM

Following the notation of Ref. [8], the most general form for the virtual photoabsorption cross section in the center-of-mass frame (c.m.) from an unpolarized target, allowing for both a polarized electron beam and recoil hyperon, is given by:

$$\begin{aligned} \frac{d\sigma_v}{d\Omega_K^*} = & \mathcal{K} \sum_{\beta=0, x', y', z'} \left(R_T^{\beta 0} + \epsilon_L R_L^{\beta 0} + c_+ ({}^c R_{LT}^{\beta 0} \cos \Phi + {}^s R_{LT}^{\beta 0} \sin \Phi) \right. \\ & + \epsilon ({}^c R_{TT}^{\beta 0} \cos 2\Phi + {}^s R_{TT}^{\beta 0} \sin 2\Phi) \\ & \left. + hc_- ({}^c R_{LT'}^{\beta 0} \cos \Phi + {}^s R_{LT'}^{\beta 0} \sin \Phi) + hc_0 R_{TT'}^{\beta 0} \right). \end{aligned} \quad (1)$$

The $R_i^{\beta\alpha}$ are the transverse, longitudinal, and interference response functions that relate to the underlying hadronic current and implicitly contain the Λ polarization. The sum over β includes contributions from the hyperon polarization with respect to the (x', y', z') axes. In this system, \hat{z}' is along the outgoing K^+ direction, \hat{y}' is normal to the hadronic reaction plane, and $\hat{x}' = \hat{y}' \times \hat{z}'$ (Fig. 1). The $\beta = 0$ terms account for the unpolarized response and $\alpha=0$ implies an unpolarized target. The response functions denoted by $R_{LT'}$ and $R_{TT'}$ depend on the electron beam helicity h . The left superscripts on the response functions, c or s , indicate whether the term multiplies a sine or cosine term, respectively.

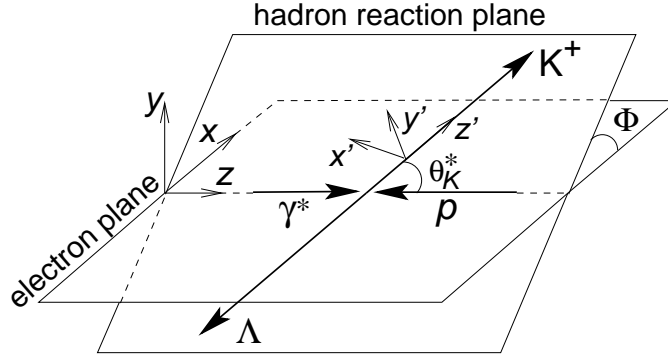


FIG. 1: Kinematics for $K^+\Lambda$ electroproduction showing angles and polarization axes in the center-of-mass reference frame.

The kinematic terms are defined by $c_{\pm} = \sqrt{2\epsilon_L(1 \pm \epsilon)}$ and $c_0 = \sqrt{1 - \epsilon^2}$, with the transverse and longitudinal polarization of the virtual photon defined respectively as $\epsilon = [1 + 2(1 + \nu^2/Q^2) \tan^2 \theta_e/2]^{-1}$ and $\epsilon_L = \epsilon Q^2/(k_{\gamma}^{c.m.})^2$. Here θ_e is the electron scattering angle, Q^2 is the negative of the four-momentum-transfer squared, ν is the virtual photon energy, and $k_{\gamma}^{c.m.}$ is the virtual-photon c.m. momentum. The leading factor $\mathcal{K} = |\vec{q}_K|/k_{\gamma}^{c.m.}$, where \vec{q}_K is the kaon c.m. momentum.

Using Eq.(1), the helicity-dependent hyperon polarization components, P' , in the (x', y', z') system are given by [1, 9]:

$$\begin{aligned}\sigma_0 P'_{x'} &= \mathcal{K}(c_- {}^c R_{LT'}^{x'0} \cos \Phi + c_0 R_{TT'}^{x'0}), \\ \sigma_0 P'_{y'} &= \mathcal{K} c_- {}^s R_{LT'}^{y'0} \sin \Phi, \\ \sigma_0 P'_{z'} &= \mathcal{K}(c_- {}^c R_{LT'}^{z'0} \cos \Phi + c_0 R_{TT'}^{z'0}).\end{aligned}\tag{2}$$

Here, σ_0 represents the unpolarized part of the cross section, which can be defined in terms of either response functions R_i or structure functions σ_i as:

$$\begin{aligned}\sigma_0 \equiv \frac{d\sigma_v}{d\Omega_K^*} &= \mathcal{K} \left[R_T^{00} + \epsilon_L R_L^{00} + \sqrt{2\epsilon_L(1+\epsilon)} {}^c R_{LT}^{00} \cos \Phi + \epsilon {}^c R_{TT}^{00} \cos 2\Phi \right] \\ &= \sigma_T + \epsilon \sigma_L + \sqrt{2\epsilon(1+\epsilon)} \sigma_{LT} \cos \Phi + \epsilon \sigma_{TT} \cos 2\Phi,\end{aligned}\tag{3}$$

where we note that $\sigma_T = \mathcal{K} R_T^{00}$ and $\epsilon \sigma_L = \mathcal{K} \epsilon_L R_L^{00}$.

The transferred polarization can also be defined in the (x, y, z) coordinate system where \hat{z} is along the virtual photon direction, \hat{y} is normal to the electron scattering plane, and $\hat{x} = \hat{y} \times \hat{z}$ (see Fig. 1). The components of P' in the (x, y, z) system are related to those in the (x', y', z') system by a simple rotation and are given by:

$$\begin{aligned}P'_x &= P'_{x'} \cos \Phi \cos \theta_K^* - P'_{y'} \sin \Phi + P'_{z'} \cos \Phi \sin \theta_K^* \\ P'_y &= P'_{x'} \sin \Phi \cos \theta_K^* + P'_{y'} \cos \Phi + P'_{z'} \sin \Phi \sin \theta_K^* \\ P'_z &= -P'_{x'} \sin \theta_K^* + P'_{z'} \cos \theta_K^*,\end{aligned}\tag{4}$$

where θ_K^* is the K^+ c.m. polar angle defined in Fig. 1.

The polarization transfer data of Ref. [1] were summed over all Φ angles to accommodate finite bin sizes and to improve statistics. The resulting Φ -integrated transferred polarization components, \mathcal{P}' , for the two coordinate systems become:

$$\mathcal{P}'_{x'} = \frac{c_0 R_{TT'}^{x'0}}{R_T^{00} + \epsilon_L R_L^{00}}, \quad \mathcal{P}'_{z'} = \frac{c_0 R_{TT'}^{z'0}}{R_T^{00} + \epsilon_L R_L^{00}}\tag{5}$$

and

$$\begin{aligned}\mathcal{P}'_x &= \frac{c_- ({}^c R_{LT'}^{x'0} \cos \theta_K^* - R_{LT'}^{y'0} + {}^s R_{LT'}^{z'0} \sin \theta_K^*)}{R_T^{00} + \epsilon_L R_L^{00}}, \\ \mathcal{P}'_z &= \frac{c_0 (-R_{TT'}^{x'0} \sin \theta_K^* + R_{TT'}^{z'0} \cos \theta_K^*)}{R_T^{00} + \epsilon_L R_L^{00}}.\end{aligned}\tag{6}$$

The components of \mathcal{P}' along the \hat{y} and \hat{y}' axes are identically zero from the integration of Eqs.(2) and (4) over $0 \leq \Phi \leq 2\pi$. Concentrating now on the z' and z components in parallel or anti-parallel kinematics ($\cos \theta_K^* = \pm 1$), Eqs.(5) and (6) reduce to:

$$\mathcal{P}'_{z'} = \pm \mathcal{P}'_z = \pm \frac{c_0 R_{TT'}^{z'0}}{R_T^{00} + \epsilon_L R_L^{00}}, \quad (7)$$

where the plus (minus) sign is associated with the parallel (anti-parallel) kinematics case.

The response functions of Eq.(7) can be written in terms of the CGLN amplitudes [10] as shown in Ref. [8] as:

$$R_{TT'}^{z'0} = \text{Re} \left[-2F_1^* F_2 + \cos \theta_K^* (|F_1|^2 + |F_2|^2) - \sin^2 \theta_K^* (F_1^* F_3 + F_2^* F_4) \right], \quad (8)$$

$$R_T^{00} = |F_1|^2 + |F_2|^2 + \frac{\sin^2 \theta_K^*}{2} (|F_3|^2 + |F_4|^2) \\ + \text{Re} \left[\sin^2 \theta_K^* (F_2^* F_3 + F_1^* F_4 + \cos \theta_K^* F_3^* F_4) - 2 \cos \theta_K^* F_1^* F_2 \right], \quad (9)$$

$$R_L^{00} = \text{Re} \left[|F_5|^2 + |F_6|^2 + 2 \cos \theta_K^* F_5^* F_6 \right]. \quad (10)$$

For the case of $\theta_K^* = 0$, these forms simplify to:

$$R_{TT'}^{z'0} = R_T^{00} = |F_1 - F_2|^2 \quad \text{and} \quad R_L^{00} = |F_5 + F_6|^2. \quad (11)$$

Combining the result of Eq.(11) with Eq.(7) we obtain:

$$\mathcal{P}'_{z'} = \mathcal{P}'_z = \frac{c_0 R_T^{00}}{R_T^{00} + \epsilon_L R_L^{00}}.$$

This expression can then be inverted to determine the ratio of the longitudinal to transverse response functions [9], or alternatively, the ratio of $R_\sigma = \sigma_L/\sigma_T$ as:

$$R_\sigma = \frac{\sigma_L}{\sigma_T} = \frac{1}{\epsilon} \left(\frac{c_0}{\mathcal{P}'_{z'}} - 1 \right). \quad (12)$$

III. EXTRACTION OF R_σ

Figure 2 reproduces the results from Ref. [1] along with sample model calculations. The kinematic values and the most forward-angle data points are given in Table I. The curves correspond to the hydrodynamic models of Refs. [3] (solid), and [4] (dashed) and have been averaged over the kinematical bins. It is clear that the models badly miss in predicting polarization at nearly all values of $\cos \theta_K^*$ and, therefore, must fail to predict R_σ .

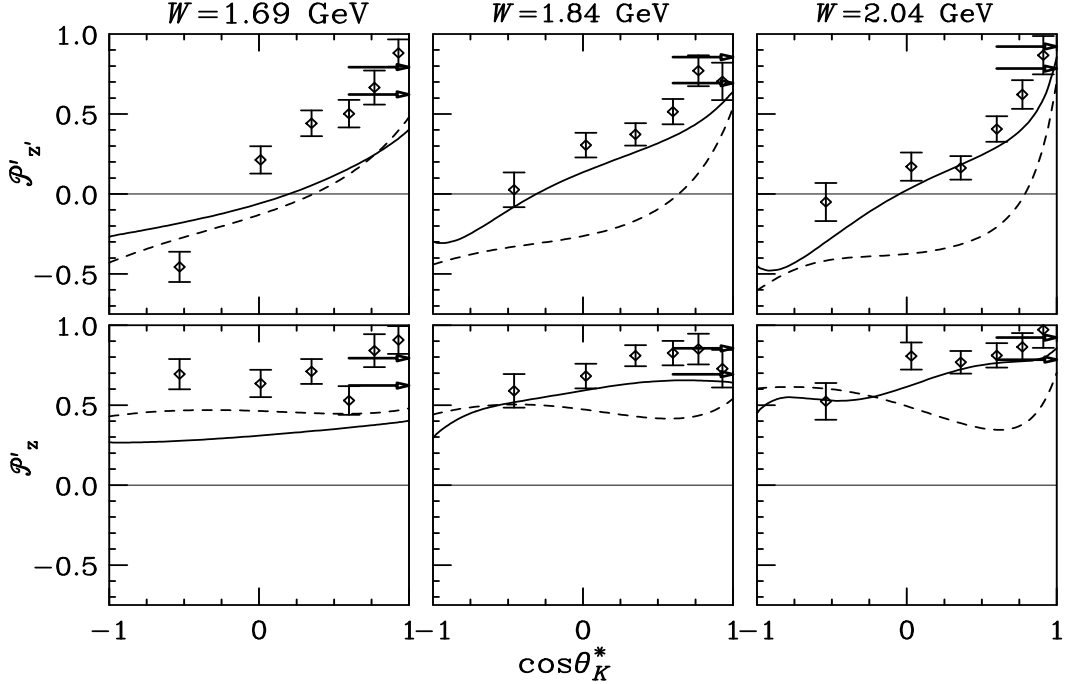


FIG. 2: Transferred Λ polarization projected along the z' (top) and z (bottom) axes versus $\cos\theta_K^*$ from Ref. [1]. The data were summed over Q^2 and Φ and are shown for three central values of W as indicated. The solid and dashed curves correspond to the hydrodynamic models of Refs. [3] and [4], respectively. The upper arrow in each plot indicates the maximum physically allowable value of the polarization at $\cos\theta_K^* = 1$, while the lower arrows indicate the polarization corresponding to $R_\sigma = 0.45$.

Since both R_L^{00} and R_T^{00} must be positive definite, Eq.(12) gives a maximum value of $\mathcal{P}'_{z'} = \mathcal{P}'_z = c_0$ at $\cos\theta_K^* = 1$. This limiting value is shown by the upper arrow in each plot of Fig. 2. This arises from the fact that these response functions can be written in terms of absolute squares of helicity amplitudes, as shown in Ref. [8], and must therefore always be greater than zero.

The small-angle data of Ref. [1] cover an angular bin of $0.8 \leq \cos\theta_K^* \leq 1$ and therefore do not give direct access to $\mathcal{P}'_{z'}$ or \mathcal{P}'_z at $\cos\theta_K^* = 1$. However, the values of the polarization in the smallest angle bins and the trends of the data reveal a marked difference from what is expected given the recent R_σ results of Mohring *et al.* [5]. The three Mohring data points at $Q^2=0.52, 0.75,$ and 1.00 GeV² and $W=1.84$ GeV give an approximate average value of $R_\sigma = 0.45$. This would give polarizations at $\cos\theta_K^* = 1$ shown by the lower arrows in the plots of Fig. 2 and also given in the last column of Table I. It is clear that the Mohring

$\langle W \rangle$ GeV	$\langle Q^2 \rangle$ GeV ²	$\langle \epsilon \rangle$	$\mathcal{P}'_{z'} \pm \Delta \mathcal{P}'_{z'}$	$\mathcal{P}'_z \pm \Delta \mathcal{P}'_z$	$\mathcal{P}'_{z'}(x = 1)$
1.69	0.77	0.609	0.881±0.086	0.907±0.087	0.62
1.84	0.69	0.518	0.704±0.116	0.728±0.118	0.69
2.03	0.61	0.388	0.868±0.120	0.971±0.114	0.78

TABLE I: Transferred polarization data at $\cos \theta_K^* = 0.93$ from Ref. [1] at average kinematic quantities as shown. The Q^2 range extends from 0.35 up to 1.4, 1.2, and 1.0 GeV² for the kinematic bins, respectively. The last column gives the values of $\mathcal{P}'_{z'}$ and \mathcal{P}'_z at $x \equiv \cos \theta_K^* = 1$ for a ratio of $R_\sigma = 0.45$ —the approximate average value from Ref. [5].

results lead to a much lower value for the polarization at $\cos \theta_K^* = 1$ than the trends of the polarization data at both $W=1.69$ and 2.04 GeV indicate.

While the qualitative discussion above is useful in setting the stage, a reliable extrapolation of the \mathcal{P}' polarization data to $\cos \theta_K^* = 1$ is needed to determine R_σ . This can be done by fitting the $\cos \theta_K^*$ dependence of the polarization data. Besides the explicit θ_K^* dependence of \mathcal{P}' noted in Eq.(6) and the response functions of Eqs.(8-10), the CGLN amplitudes contain additional θ_K^* dependence (as well as Q^2 and W dependence). This suggests that the polarizations be fit with a ratio of polynomials in $x = \cos \theta_K^*$. The number of terms is governed by the reaction dynamics. However, given the limited number of polarization data points, the number of terms in any fit leading to a meaningful extrapolation to $\cos \theta_K^* = 1$ must also be limited. We considered fits of the form:

$$\mathcal{P}'_{z'} = \frac{a_1 + a_2x + a_3x^2 + a_4^3}{b_1 + b_2x + b_3x^2 + b_4x^3} \quad (13)$$

$$\mathcal{P}'_z = \frac{c_1 + c_2x + c_3x^2}{b_1 + b_2x + b_3x^2 + b_4x^3}. \quad (14)$$

Eq.(7) provides constraints that reduce the number of free parameters enabling us to rewrite Eq.(14) as

$$\mathcal{P}'_z = \frac{(a_2 + a_4 - c_3) + (a_1 + a_3)x + c_3x^2}{b_1 + b_2x + b_3x^2 + b_4x^3}. \quad (15)$$

We have additional information that helps us to constrain the terms in the denominator. This comes from the unpublished $p(e, e'K^+)\Lambda$ cross section data from CLAS of Feuerbach [12]. In that work, the polarization-independent cross sections of Eq.(3) were measured over $0 \leq \Phi \leq 2\pi$. A fit to the Φ dependence thus enabled the extraction of the

structure functions of Eq.(3): $\sigma_u \equiv \sigma_T + \epsilon\sigma_L$, σ_{LT} , and σ_{TT} . Since σ_u is proportional to our denominator, we can fit

$$\sigma_u = b_1 + b_2x + b_3x^2 + b_4x^3. \quad (16)$$

Feuerbach's data is at slightly different values of W and Q^2 than the polarization data. However, we will demonstrate that the fits and the extrapolations to $\cos\theta_K^* = 1$ are not very sensitive to the precise shape of σ_u .

A simultaneous fit of Eqs.(13), (15), and (16) to the polarization data and σ_u allows us to determine the fit parameters and to extrapolate the polarizations to $\cos\theta_K^* = 1$. For the $W=1.69$ and 1.84 GeV data, we found that \mathcal{P}'_z could be fit without the cubic term in the numerator ($a_4 = 0$), resulting in eight free parameters. The polarization data at $W=2.04$ GeV required the cubic term. Fig. 3 shows the resulting fits of the polarization data.

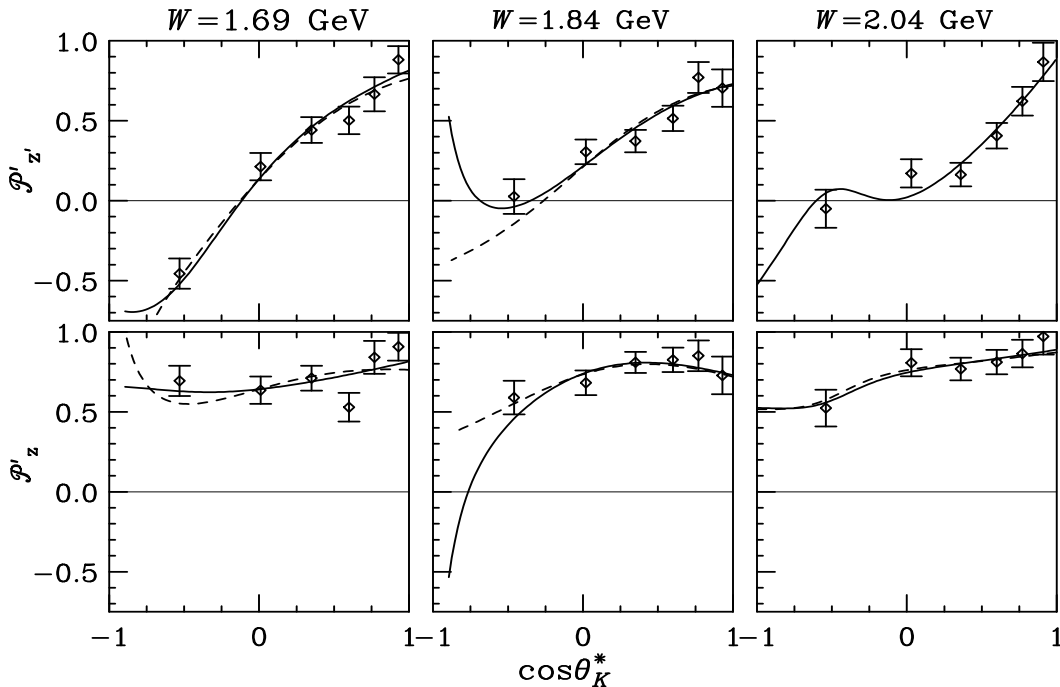


FIG. 3: Transferred Λ polarization versus $\cos\theta_K^*$ from Ref. [1] along with our fits. The different curves are described in the text.

There are two curves shown for the $W=1.84$ GeV data. The solid curve is the result of allowing the fitting routine—a variation of the Levenberg-Marquardt method [13]—to find the minimum χ^2 (labeled Fit 2a in Table II). This results in a fit that clearly gives unphysical values of $\mathcal{P}'_z > 1$ and $\mathcal{P}'_z < -1$ at $\cos\theta_K^* = -1$. The dashed curve (Fit 2b) is the result of a

$\langle W \rangle$ GeV	$\langle Q^2 \rangle$ GeV ²	Fit	$\chi^2/\text{pt.}$	$\mathcal{P}'_z(x=1)$	R_σ
1.69	0.77	1a	1.03	0.815±0.057	-0.044±0.113
		1b	1.30	0.763±0.056	0.065±0.127
1.84	0.69	2a	0.66	0.729±0.064	0.333±0.200
		2b	0.80	0.720±0.064	0.364±0.203
2.04	0.61	3a	0.54	0.888±0.086	0.097±0.260
		3b	0.28	0.872±0.103	0.148±0.320

TABLE II: Transferred polarization at $x = \cos\theta_K^* = 1.0$ extrapolated from fits described in the text along with the resulting value of the ratio of transverse to longitudinal structure functions. Uncertainties are statistical uncertainties arising from the fitting procedure.

similar fit that forced the polarization at $\cos\theta_K^* = -1$ to a physically allowable value. The overall χ^2 -per-point for the polarization data did not change significantly, while yielding a more physically sensible fit. More importantly, the value of the extrapolated polarization at $\cos\theta_K^* = 1$ (also given in Table II) does not change significantly. This is telling us that the fit at forward angles is essentially unaffected by the fact that it is poorly constrained at back angles.

The solid curves (Fit 3a) shown for the $W=2.04$ GeV data are the result of the nine-parameter fit ($a_4 \neq 0$). The dashed curve in the lower panel (Fit 3b) is the result of fitting only \mathcal{P}'_z and σ_u (seven parameters). We see very little difference in the curves, however, we get a much larger uncertainty in the extrapolated polarization for the latter fit.

Finally, to show that we are largely insensitive to the exact form of the cross section data, we show two different fits to the data at $W=1.69$ GeV. The solid curve is the result of the nominal fit (Fit 1a). For the dashed curve (Fit 1b), we used σ_u data for $W=1.84$ GeV instead of $W=1.69$ GeV. This results in a fit that again gives unphysical values of the polarizations at $\cos\theta_K^* = -1$. Despite this obvious shortcoming, we get a very similar result for the extrapolation to $\cos\theta_K^* = 1$. This tells us that the fits to the polarization data are not terribly sensitive to the precise shape of the cross section data.

Plugging the extrapolated polarizations into Eq.(12) we can determine the ratio R_σ . These values are shown in the last column of Table II along with the corresponding statistical

uncertainties determined by the fit. At a single kinematic point, the variation in R_σ for the different fits is small compared to the statistical uncertainty. This is even true in the worst case where we have used an obviously wrong cross section (Fit 1b). We estimate therefore, an absolute systematic error of less than 0.1 due to the fitting procedure and possible systematic uncertainties in the cross section data. Ref. [1] cites an absolute systematic error of less than 0.08 for each polarization point. This increases the uncertainty in R_σ by approximately 0.05. We estimate the combined systematic uncertainty in R_σ to be less than 0.11.

IV. DISCUSSION

The resulting values for R_σ (Fits 1a, 2a, and 3a) are plotted in Fig. 4. For comparison, we have also included the previous world's data [5, 6, 7]. We see that results are much smaller than the previous data obtained using the more common Rosenbluth separation method. In this method, the unpolarized cross section at a given Q^2 and W is measured in parallel kinematics as a function of ϵ . The cross section reduces to $\sigma_u = \sigma_T + \epsilon\sigma_L$. In principle, fitting the cross section data with a straight line gives σ_L and σ_T . However, this technique relies on a very precise determination of the absolute cross section at all ϵ points. To illustrate the inherent difficulties of this technique one only needs to compare the results of Mohring [5] with those of Niculescu [7]. These are two analyses of the same data set taken in Hall C of Jefferson Lab. The Mohring results were published later and are generally believed to be more reliable. These data were measured at $W=1.84$ GeV—the same as our middle data point. Our own results not only seem to rule out the Niculescu results, but probably also the Mohring results. It seems unlikely that the small differences in W (≤ 200 MeV) can account for the observed discrepancy.

Our result implies a very small longitudinal structure function and hence a small longitudinal coupling of the virtual photon. This structure function is expected to be very sensitive to the kaon form factor [14]. A recently conducted experiment in Hall A at Jefferson Laboratory [15] has as one of its main goals a Rosenbluth separation at several values of momentum transfer t leading to a Chew-Low [16] extrapolation of the kaon form factor. However, this method relies on having small *relative* uncertainties for σ_L . Therefore, if σ_L is as small as our results indicate, it seems unlikely that a reliable determination of the kaon form factor can be performed in these kinematics.

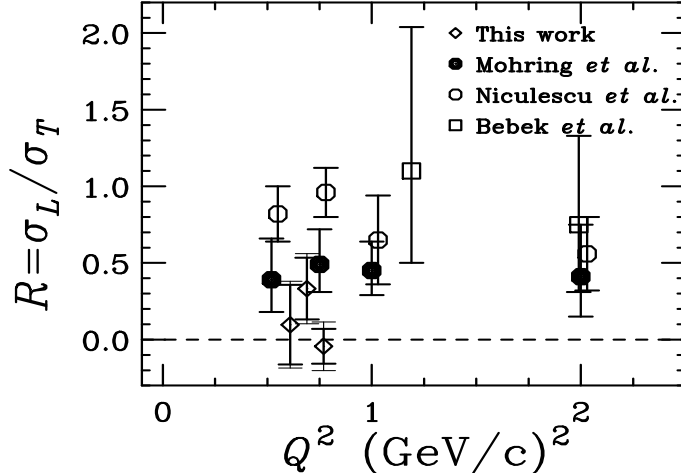


FIG. 4: Ratio of longitudinal to transverse structure functions vs. Q^2 . The inner error bars on the diamonds indicate our statistical uncertainties; the outer bars reflect the quadratic sum of statistical and estimated systematic errors. The Niculescu results [7], which were superseded by the Mohring results [5], are offset in Q^2 for clarity.

This is not the first significant discrepancy between Rosenbluth and polarization-transfer results. The ratio of the proton’s electric and magnetic form factors, $\mu_p G_E/G_M$, has been measured by both Rosenbluth and polarization-transfer methods (see Ref. [17] and references therein) with a very large discrepancy. The common wisdom is that the polarization-transfer method is much less susceptible to systematic errors. If one believes that the polarization-transfer results are correct, then the slope derived from the Rosenbluth technique is too large. This is similar to what is implied by our results. One explanation that is being widely discussed is that there is an ϵ -dependent, two-photon-exchange effect that has not been properly accounted for in the radiative corrections applied to the experimental cross sections [18]. Some calculations [19] indicate that including this effect would bring down the high ϵ data points relative to the low ϵ data points and lead to better agreement between the Rosenbluth and polarization-transfer results. It is certainly premature to attribute any differences between Rosenbluth results and our polarization-transfer results for $K^+\Lambda$ electroproduction to two-photon exchange. However, it is interesting that the trend of the differences is in the same direction as observed in the $\mu_p G_E/G_M$ results.

We would like to note that the polarization transfer data from which we extracted R_σ is just the first to come out of a larger program of kaon electroproduction in Jefferson Lab’s Hall B [20]. Analysis is currently underway in which cross sections and polarization

observables will be measured covering W from threshold up to 3.0 GeV and Q^2 from 0.4 up to 5 GeV². These data will yield a factor of 4 better statistical uncertainty for the Λ polarization transfer, thus leading to a more reliable determination of R_σ . In addition, Hall B will produce its own Rosenbluth separation that will complement both the existing data and results that are expected soon from Hall A [15]. We are eager to see if the discrepancies between the two techniques of extracting R_σ hold up with the coming results.

In conclusion, we have done the first extraction of the ratio $R_\sigma = \sigma_L/\sigma_T$ from transferred polarization data for the $p(\vec{e}, e'K^+)\vec{\Lambda}$ reaction. Our results are significantly different from results obtained by the Rosenbluth technique and are also significantly different from model predictions. These results indicate a very small longitudinal structure function for Q^2 of around 0.7 GeV² and W of 1.69, 1.84, and 2.04 GeV.

-
- [1] D.S. Carman *et al.*, Phys. Rev. Lett. **90**, 131804 (2003).
 - [2] C. Bennhold and S. Janssen, private communications.
 - [3] T. Mart and C. Bennhold, Phys. Rev. C **61**, 012201 (2000); H. Habermehl *et al.*, Phys. Rev. C **58**, R40 (1998).
 - [4] S. Janssen *et al.*, Phys. Rev. C **65**, 015201 (2002).
 - [5] R.M. Moring *et al.*, Phys. Rev. C **67**, 055205 (2003).
 - [6] C.J. Bebek *et al.*, Phys. Rev. D **15**, 3082 (1977).
 - [7] G. Niculescu *et al.*, Phys. Rev. Lett. **81**, 1805 (1998).
 - [8] G. Knöchlein, D. Dreschel, and L. Tiator, Z. Phys. A **352**, 327 (1995).
 - [9] H. Schmieden and L. Tiator, Eur. Phys. J. A **8**, 15 (2000).
 - [10] G.F. Chew *et al.*, Phys. Rev. **106**, 1345 (1957).
 - [11] H. Schmieden, Eur. Phys. J. A **1**, 427 (1998).
 - [12] Robert Feuerbach, Ph.D. Dissertation, Carnegie Mellon University, 2002.
 - [13] William H. Press, Brian P. Flannery, Saul A. Teukolsky, and William T. Vetterling, *Numerical Recipes: The Art of Scientific Computing* (Cambridge University Press, Cambridge, 1986).
 - [14] B. Saghai, Nucl. Phys. **A639**, 217 (1998).
 - [15] P. Markowitz *et al.*, Jefferson Lab experiment E94-108.
 - [16] William R. Frazer, Phys. Rev **115**, 1763 (1959).

- [17] J. Arrington, Phys. Rev. C **68**, 034325 (2003).
- [18] J. Arrington, Pre-print nucl-ex/0311019.
- [19] P.G. Blunden, W. Melnitchouk, and J.A. Tjon, Pre-print nucl-th/0306076.
- [20] D.S. Carman *et al.*, Jefferson Lab experiments E99-006 and E00-112; K.H. Hicks *et al.*, Jefferson Lab experiment E93-030.